

Measures of star formation rates from Infrared (*Herschel*) and ultraviolet (*GALEX*) emissions of galaxies 1

## Measures of star formation rates from Infrared (*Herschel*) and UV (*GALEX*) emissions of galaxies in the HerMES fields

V. Buat,<sup>1\*</sup> E. Giovannoli,<sup>1</sup> D. Burgarella,<sup>1</sup> B. Altieri,<sup>2</sup> A. Amblard,<sup>3</sup> V. Arumugam,<sup>4</sup> H. Aussel,<sup>5</sup> T. Babbedge,<sup>6</sup> A. Blain,<sup>7</sup> J. Bock,<sup>7,8</sup> A. Boselli,<sup>1</sup> N. Castro-Rodríguez,<sup>9,10</sup> A. Cava,<sup>9,10</sup> P. Chanial,<sup>6</sup> D.L. Clements,<sup>6</sup> A. Conley,<sup>11</sup> L. Conversi,<sup>2</sup> A. Cooray,<sup>3,7</sup> C.D. Dowell,<sup>7,8</sup> E. Dwek,<sup>12</sup> S. Eales,<sup>13</sup> D. Elbaz,<sup>5</sup> M. Fox,<sup>6</sup> A. Franceschini,<sup>14</sup> W. Gear,<sup>13</sup> J. Glenn,<sup>11</sup> M. Griffin,<sup>13</sup> M. Halpern,<sup>15</sup> E. Hatziminaoglou,<sup>16</sup> S. Heinis,<sup>1</sup> E. Ibar,<sup>17</sup> K. Isaak,<sup>13</sup> R.J. Ivison,<sup>17,4</sup> G. Lagache,<sup>18</sup> L. Levenson,<sup>7,8</sup> C.J. Lonsdale,<sup>19</sup> N. Lu,<sup>7,20</sup> S. Madden,<sup>5</sup> B. Maffei,<sup>21</sup> G. Magdis,<sup>5</sup> G. Mainetti,<sup>14</sup> L. Marchetti,<sup>14</sup> G.E. Morrison,<sup>22,23</sup> H.T. Nguyen,<sup>8,7</sup> B. O'Halloran,<sup>6</sup> S.J. Oliver,<sup>24</sup> A. Omont,<sup>25</sup> F.N. Owen,<sup>19</sup> M.J. Page,<sup>26</sup> M. Pannella,<sup>19</sup> P. Panuzzo,<sup>5</sup> A. Papageorgiou,<sup>13</sup> C.P. Pearson,<sup>27,28</sup> I. Pérez-Fournon,<sup>9,10</sup> M. Pohlen,<sup>13</sup> D. Rigopoulou,<sup>27,29</sup> D. Rizzo,<sup>6</sup> I.G. Roseboom,<sup>24</sup> M. Rowan-Robinson,<sup>6</sup> M. Sánchez Portal,<sup>2</sup> B. Schulz,<sup>7,20</sup> N. Seymour,<sup>26</sup> D.L. Shupe,<sup>7,20</sup> A.J. Smith,<sup>24</sup> J.A. Stevens,<sup>30</sup> V. Strazzullo,<sup>19</sup> M. Symeonidis,<sup>26</sup> M. Trichas,<sup>6</sup> K.E. Tugwell,<sup>26</sup> M. Vaccari,<sup>14</sup> E. Valiante,<sup>15</sup> I. Valtchanov,<sup>2</sup> L. Vigroux,<sup>25</sup> L. Wang,<sup>24</sup> R. Ward,<sup>24</sup> G. Wright,<sup>17</sup> C.K. Xu<sup>7,20</sup> and M. Zemcov<sup>7,8</sup>

<sup>1</sup>Laboratoire d'Astrophysique de Marseille, OAMP, Université Aix-marseille, CNRS, 38 rue Frédéric Joliot-Curie, 13388 Marseille cedex 13, France

<sup>2</sup>Herschel Science Centre, European Space Astronomy Centre, Villanueva de la Cañada, 28691 Madrid, Spain

<sup>3</sup>Dept. of Physics & Astronomy, University of California, Irvine, CA 92697, USA

<sup>4</sup>Institute for Astronomy, University of Edinburgh, Royal Observatory, Blackford Hill, Edinburgh EH9 3HJ, UK

<sup>5</sup>Laboratoire AIM-Paris-Saclay, CEA/DSM/Irfu - CNRS - Université Paris Diderot, CE-Saclay, pt courrier 131, F-91191 Gif-sur-Yvette, France

<sup>6</sup>Astrophysics Group, Imperial College London, Blackett Laboratory, Prince Consort Road, London SW7 2AZ, UK

<sup>7</sup>California Institute of Technology, 1200 E. California Blvd., Pasadena, CA 91125, USA

<sup>8</sup>Jet Propulsion Laboratory, 4800 Oak Grove Drive, Pasadena, CA 91109, USA

<sup>9</sup>Instituto de Astrofísica de Canarias (IAC), E-38200 La Laguna, Tenerife, Spain

<sup>10</sup>Departamento de Astrofísica, Universidad de La Laguna (ULL), E-38205 La Laguna, Tenerife, Spain

<sup>11</sup>Dept. of Astrophysical and Planetary Sciences, CASA 389-UCB, University of Colorado, Boulder, CO 80309, USA

<sup>12</sup>Observational Cosmology Lab, Code 665, NASA Goddard Space Flight Center, Greenbelt, MD 20771, USA

<sup>13</sup>Cardiff School of Physics and Astronomy, Cardiff University, Queens Buildings, The Parade, Cardiff CF24 3AA, UK

<sup>14</sup>Dipartimento di Astronomia, Università di Padova, vicolo Osservatorio, 3, 35122 Padova, Italy

<sup>15</sup>Department of Physics & Astronomy, University of British Columbia, 6224 Agricultural Road, Vancouver, BC V6T 1Z1, Canada

<sup>16</sup>ESO, Karl-Schwarzschild-Str. 2, 85748 Garching bei München, Germany

<sup>17</sup>UK Astronomy Technology Centre, Royal Observatory, Blackford Hill, Edinburgh EH9 3HJ, UK

<sup>18</sup>Institut d'Astrophysique Spatiale (IAS), bâtiment 121, Université Paris-Sud 11 and CNRS (UMR 8617), 91405 Orsay, France

<sup>19</sup>National Radio Astronomy Observatory, P.O. Box O, Socorro NM 87801, USA

<sup>20</sup>Infrared Processing and Analysis Center, MS 100-22, California Institute of Technology, JPL, Pasadena, CA 91125, USA

<sup>21</sup>School of Physics and Astronomy, The University of Manchester, Alan Turing Building, Oxford Road, Manchester M13 9PL, UK

<sup>22</sup>Institute for Astronomy, University of Hawaii, Honolulu, HI 96822, USA

<sup>23</sup>Canada-France-Hawaii Telescope, Kamuela, HI, 96743, USA

<sup>24</sup>Astronomy Centre, Dept. of Physics & Astronomy, University of Sussex, Brighton BN1 9QH, UK

<sup>25</sup>Institut d'Astrophysique de Paris, UMR 7095, CNRS, UPMC Univ. Paris 06, 98bis boulevard Arago, F-75014 Paris, France

<sup>26</sup>Mullard Space Science Laboratory, University College London, Holmbury St. Mary, Dorking, Surrey RH5 6NT, UK

<sup>27</sup>Space Science & Technology Department, Rutherford Appleton Laboratory, Chilton, Didcot, Oxfordshire OX11 0QX, UK

<sup>28</sup>Institute for Space Imaging Science, University of Lethbridge, Lethbridge, Alberta, T1K 3M4, Canada

<sup>29</sup>Astrophysics, Oxford University, Keble Road, Oxford OX1 3RH, UK

<sup>30</sup>Centre for Astrophysics Research, University of Hertfordshire, College Lane, Hatfield, Hertfordshire AL10 9AB, UK

**ABSTRACT**

The reliability of infrared (IR) and ultraviolet (UV) emissions to measure star formation rates in galaxies is investigated for a large sample of galaxies observed with the SPIRE and PACS instruments on *Herschel* as part of the HerMES project. We build flux-limited 250  $\mu\text{m}$  samples of sources at redshift  $z < 1$ , cross-matched with the *Spitzer*/MIPS and *GALEX* catalogues. About 60 % of the *Herschel* sources are detected in UV. The total IR luminosities,  $L_{\text{IR}}$ , of the sources are estimated using a SED-fitting code that fits to fluxes between 24 and 500  $\mu\text{m}$ . Dust attenuation is discussed on the basis of commonly-used diagnostics: the  $L_{\text{IR}}/L_{\text{UV}}$  ratio and the slope,  $\beta$ , of the UV continuum. A mean dust attenuation  $A_{\text{UV}}$  of  $\simeq 3$  mag is measured in the samples.  $L_{\text{IR}}/L_{\text{UV}}$  is found to correlate with  $L_{\text{IR}}$ . Galaxies with  $L_{\text{IR}} > 10^{11}L_{\odot}$  and  $0.5 < z < 1$  exhibit a mean dust attenuation  $A_{\text{UV}}$  about 0.7 mag lower than that found for their local counterparts, although with a large dispersion. Our galaxy samples span a large range of  $\beta$  and  $L_{\text{IR}}/L_{\text{UV}}$  values which, for the most part, are distributed between the ranges defined by the relations found locally for starburst and normal star-forming galaxies. As a consequence the recipe commonly applied to local starbursts is found to overestimate the dust attenuation correction in our galaxy sample by a factor  $\sim 2 - 3$ . The SFRs deduced from  $L_{\text{IR}}$  are found to account for about 90% of the total SFR; this percentage drops to 71% for galaxies with  $\text{SFR} < 1M_{\odot}\text{yr}^{-1}$  (or  $L_{\text{IR}} < 10^{10}L_{\odot}$ ). For these faint objects, one needs to combine UV and IR emissions to obtain an accurate measure of the SFR.

**Key words:** galaxies: evolution-galaxies: stellar content-infrared: galaxies-ultraviolet: galaxies

**1 INTRODUCTION**

Far-infrared (IR) and ultraviolet (UV) luminosities are commonly used to estimate the current star formation rate (SFR) in galaxies since both emissions are expected to come from young stars. By combining observed IR and UV luminosities one can therefore make an energetic budget and derive an accurate measure of the total SFR in star-forming galaxies (e.g. Iglesias-Páramo et al. 2004; Elbaz et al. 2007). It is often the case that only UV or IR data exist, however, and so the question remains of how reliably one can determine SFRs from UV or IR alone.

SFRs derived from dust emission are based on estimates of the total IR luminosity ( $L_{\text{IR}} = L[8 - 1000\mu\text{m}]$ ). This measure is accurate in the nearby Universe thanks to the observations of *IRAS* and *Spitzer*, both of which sampled the wavelength range close to the peak emission of the dust. *Spitzer* was also used to observe galaxies up to  $z \approx 2$  in the mid-IR, however extrapolation to the total IR luminosity remains uncertain and relies on relations determined from nearby galaxy populations. By observing in the rest-frame far-infrared of galaxies, *Herschel* (Pilbratt et al. 2010)<sup>1</sup> allows us to measure accurately this IR bolometric luminosity over a continuous and wide range of redshift.

The main issue when using UV emission to estimate SFRs is the effect of dust attenuation. The  $L_{\text{IR}}/L_{\text{UV}}$  ratio has been identified as a very powerful estimator of dust attenuation in star forming galaxies (e.g. Gordon et al. 2000; Buat et al. 2005). Dust attenuation diagnostics based on UV data

alone must be used when UV and IR rest-frame data are not simultaneously available. Meurer, Heckman, & Calzetti (1999) found a relation between the slope of the rest-frame UV continuum  $\beta$  (defined as  $f_{\lambda}(\text{erg cm}^{-2}\text{s}^{-1}\text{nm}^{-1}) \propto \lambda^{\beta}$  for  $\lambda > 120$  nm) and dust attenuation traced by  $L_{\text{IR}}/L_{\text{UV}}$  for local starburst galaxies observed by *IUE* and *IRAS*. This local starburst relation is also widely used to estimate dust attenuation in UV-selected galaxies at high redshift (Burgarella et al. 2007; Reddy et al. 2008). In the local Universe luminous IR galaxies (LIRGs with  $L_{\text{IR}} > 10^{11}L_{\odot}$ ) are found to roughly follow the local starburst law (Takeuchi et al. 2010; Howell et al. 2010); normal forming galaxies, less active in star formation than starburst ones, do not follow this relation, and the spectral slope  $\beta$  is found to depend on a number of parameters that are not solely related to dust attenuation (e.g. Buat et al. 2005; Boissier et al. 2007; Kong et al. 2004). Checking the validity of  $\beta$  as a tracer of dust attenuation on large samples of galaxies at different redshifts is therefore a key to both understanding dust attenuation processes in galaxies, and to being able to correct accurately for extinction.

In this paper we will analyse the IR and UV properties of galaxies over the redshift range,  $0 < z < 1$ . This is the first time accurate estimates of the total dust emission have been determined over a continuous range of redshift by using several IR measurements including new *Herschel* data and which can be compared to the observed UV emission.

**2 DATA**

Observations of the Lockman field were made with *Herschel* as part of the *Herschel* Multi-Tiered Extragalactic Survey

\* E-mail: veronique.buat@oamp.fr

<sup>1</sup> *Herschel* is an ESA space observatory with science instruments provided by Principal Investigator consortia. It is open for proposals for observing time from the worldwide astronomical community

(HerMES-Oliver et al. (2010))<sup>2</sup>. This field was also observed by *GALEX* (Martin et al. 2005) in FUV ( $\lambda \simeq 153$  nm) and NUV ( $\lambda \simeq 231$  nm) as part of the Deep Imaging Survey (DIS). Only sources with  $z < 1$  are detected by *GALEX* due to absorption by the Lyman Break.

Our first parent sample is based on the shallow observations of the Lockman SWIRE field (10h 45m 00s +58d 00m 00s,  $218' \times 218'$ ) with SPIRE (Griffin et al. 2010). We use the HerMES cross-identified catalogue of Roseboom et al. (2010) which is based on a linear inversion method using the positions of sources detected in the *Spitzer* 24  $\mu\text{m}$  surveys. We select 7435 sources that are detected at  $5\sigma$  or above at 250  $\mu\text{m}$ , corresponding to a limit of 23 mJy (Roseboom et al. 2010). A redshift has been assigned to 3862 sources. Where available, we use spectroscopic redshifts (taken from the NASA/IPAC Extragalactic Database), otherwise photometric redshifts from the SDSS/DR7 (Abazajian et al. 2009) and the SWIRE survey (Rowan-Robinson et al. 2008) are used by order of priority. We identify 3824 galaxies with  $z < 1$ , of which 30% have spectroscopic redshifts. This sample is then cross-matched with the *GALEX* detections in the NUV with a tolerance radius of 2 arcsec (based on *Spitzer*/IRAC coordinates): 2426 galaxies are detected in NUV with  $z < 1$ . The UV slope  $\beta$  can be calculated from the *FUV* – *NUV* colour for sources with  $z < 0.3$ . Of the 1542 objects at  $z < 0.3$ , 1250 are detected in the NUV and 943 have both FUV and NUV fluxes that are of sufficient accuracy ( $\Delta m < 0.1\text{mag}$ ) to enable reliable estimates of  $\beta$ .

Although  $\sim 40\%$  of the Lockman SWIRE sources selected at 250  $\mu\text{m}$  are not detected in the NUV it is quite difficult to study the non detections since not less than 21 *GALEX* fields with different depths are needed to cover the HerMES field. Therefore we also consider the *Herschel* deep observations of the Lockman North field (10h46m00s +59d01m00s,  $35' \times 35'$ ,  $5\sigma$  limit at 250  $\mu\text{m}$  corresponding to 8 mJy (Roseboom et al. 2010)): 70% of this field is covered by only 3 *GALEX* fields and a check of each individual source by hand is therefore possible. A second advantage of the Lockman-North field is that it was also observed with PACS (Poglitich et al. 2010) and data at 110 and 160  $\mu\text{m}$  are available. We again use the cross-matched catalogue of Roseboom et al. (2010) and perform a selection and a *GALEX* cross-match similar to that made for the Lockman SWIRE field. Photometric redshifts were determined by Strazzullo et al. (2010) from visible, NIR and IRAC data. 246 sources are selected at 250  $\mu\text{m}$ , of which 129 galaxies are detected in the NUV. The 58 sources that are considered as non-detections in the NUV are assigned a limiting magnitude of  $\text{NUV} = 24.4$  (Morissey et al. 2005). We consider as UV upper limits, objects with no *GALEX* source within 6 arcsec of the SPIRE position (for distances less than 6 arcsec the full NUV PSF falls into the 250 $\mu\text{m}$  one)).

Total IR luminosities,  $L_{\text{IR}}$ , are calculated using the CIGALE code (Noll et al. 2009) with Dale & Helou (2002) and Siebenmorgen & Krugel (2007) IR templates. A Bayesian analysis is performed to deduce physical parameters from the fitting of spectral energy distributions of galaxies. We restrict the analysis to the thermal IR ( $\geq 24\mu\text{m}$  data), and defer an analysis of the full UV-to-FIR SEDs to a later pa-

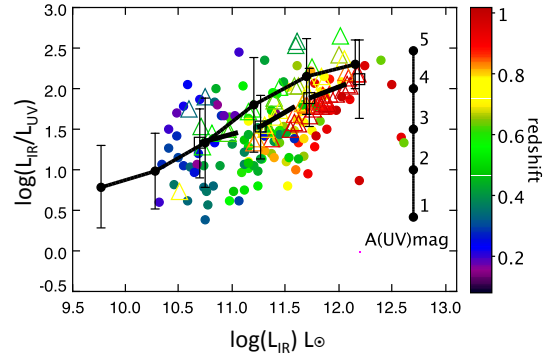


**Figure 1.**  $L_{\text{IR}}/L_{\text{UV}}$  vs.  $L_{\text{IR}}$  for sources detected in the Lockman North in the redshift range  $0 < z < 1$  (the redshift is colour-coded). Lower limits of  $L_{\text{IR}}/L_{\text{UV}}$  are plotted as triangles for galaxies not detected in UV. The filled circles and solid line correspond to the relation found for local IR selected galaxies (Buat et al. 2007a), the empty squares and dashed line to the mean values per bin of IR luminosity obtained in the present study. Errors bars correspond to the scatter of the data (1 rms). The  $A(\text{UV})$  scale is obtained using the calibration of Buat et al. (2005). The luminosity bins and mean redshift in the bins are:  $\log(L_{\text{IR}}) < 11$  and  $\langle z \rangle = 0.4$ ,  $11 \leq \log(L_{\text{IR}}) < 11.5$  and  $\langle z \rangle = 0.55$ ,  $11.5 \leq \log(L_{\text{IR}}) < 12$  and  $\langle z \rangle = 0.8$ ,  $\log(L_{\text{IR}}) \geq 12$  and  $\langle z \rangle = 0.9$ .

per. For each source we consider all the available data between 24 and 500  $\mu\text{m}$ : by construction we will always have at least two data points. We keep only objects for which the reduced chi-squared of the fit between the best template and the dataset is lower than 10 (98% of the initial samples). Typical errors on estimated  $L_{\text{IR}}$  are found lower than 0.1 dex. UV luminosities  $L_{\text{UV}}$  are derived at 153 nm rest-frame (FUV) by interpolating FUV and NUV fluxes, a mean *FUV* – *NUV* colour is used when FUV data are not available, and are defined as the quantities  $\nu L_{\nu}$ . Both  $L_{\text{IR}}$  and  $L_{\text{UV}}$  are expressed in solar units. All magnitudes are given in the AB system. We assume that  $\Omega_m = 0.3$ ,  $\Omega_{\Lambda} = 0.7$ , and  $H_0 = 70 \text{ km s}^{-1} \text{ Mpc}^{-1}$ .

### 3 DUST ATTENUATION AS TRACED BY $L_{\text{IR}}/L_{\text{UV}}$

The ratio of  $L_{\text{IR}}/L_{\text{UV}}$  is a powerful measure of dust attenuation and is known to correlate with the bolometric luminosity of galaxies in the nearby universe (e.g. Buat et al. 2007a). *Spitzer* observations extended the analysis out to  $z \simeq 0.7$  (Zheng et al. 2007; Buat et al. 2007b; Xu et al. 2007). Here we re-investigate this relation using the Lockman North sample in the redshift range  $0 < z < 1$ . We choose this field in order to be able to discuss lower limits for galaxies not detected in UV. Shown in Fig. 1 is a plot of  $L_{\text{IR}}/L_{\text{UV}}$  as a function of  $L_{\text{IR}}$ . The mean dust attenuation is  $A(\text{UV}) = 3 \pm 1 \text{ mag}$  for the whole sample (using the calibration of Buat et al. (2005)). As expected, there is a general increase of  $L_{\text{IR}}/L_{\text{UV}}$  with  $L_{\text{IR}}$ . We measure the mean  $L_{\text{IR}}/L_{\text{UV}}$  ratio within several bins of  $\log(L_{\text{IR}})$  (using the Kaplan-Meier

<sup>2</sup> hermes.sussex.ac.uk

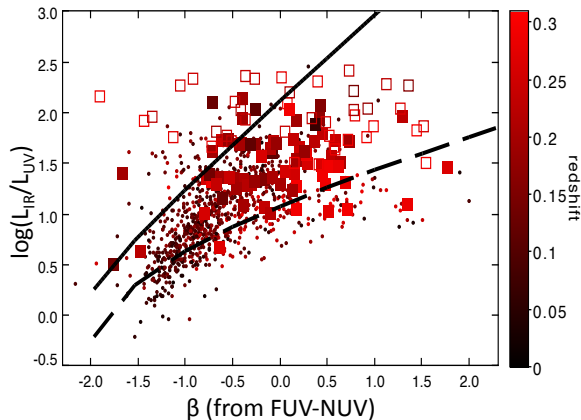


**Figure 2.**  $L_{\text{IR}}/L_{\text{UV}}$  vs.  $\beta$  (the slope of the UV continuum) for galaxies in the Lockman SWIRE field that are also detected in FUV and NUV ( $z < 0.3$ ): dots represent galaxies with  $L_{\text{IR}} < 10^{11}L_{\odot}$  and a robust measure of  $\beta$ ; filled squares represent LIRGs ( $L_{\text{IR}} > 10^{11}L_{\odot}$ ) with a robust measure of  $\beta$ , and LIRGs with less reliable  $\beta$  values are represented by empty squares. The redshift of sources is colour-coded. The superposed lines trace the relation found for local starburst galaxies (solid line) and for local normal star-forming galaxies (dashed line).

estimator to account for lower limits). The locus of galaxies at low  $z$  appears to be consistent with the  $z = 0$  relations (Buat et al. 2007a), however at  $z > 0.5$   $L_{\text{IR}}/L_{\text{UV}}$  is found to be lower by  $\sim 0.3$  dex. This difference at higher  $z$  is of low statistical significance (of the order of the  $1\sigma$  error bars) and could be affected by the lower-limit corrections but if it is real this implies a decrease in dust attenuation by  $\sim 0.7$  mag in the FUV for distant, luminous IR-selected galaxies which is consistent with dust attenuation found for LIRGs at  $z = 0.7$  by Buat et al. (2007b). A decrease in dust attenuation is possibly linked to a lower metallicity in high-redshift systems. Indeed Reddy et al. (2010) found a correlation between oxygen abundance and dust attenuation in  $z \sim 2$  star forming galaxies. The morphological evolution of LIRGs from mergers to more normal galaxies as  $z$  increases can also imply a decrease of dust attenuation (e.g. Buat et al. 2007b, and references therein). Because of a larger gas mass fraction in distant galaxies, the star formation could be spread out over larger, more diffuse and less extinguished regions than in local LIRGs. A decrease of dust attenuation was also reported by Daddi et al. (2007) for Ultraluminous IR galaxies between  $z = 0$  and  $z \sim 2$  associated to a longer lived star formation for the higher redshift sources.

#### 4 DUST ATTENUATION AS TRACED BY THE UV SLOPE

A common way to estimate dust attenuation in the UV in the absence of IR data is to use the slope  $\beta$  of the UV continuum. To estimate  $\beta$  from the  $FUV - NUV$  colour we focus on galaxies with  $z < 0.3$  in the Lockman SWIRE sample and apply the Kong et al. (2004) recipe. A measurement error of 0.1 mag in FUV and NUV translates into an error of 0.3 for  $\beta$ . Therefore we restrict the analysis (otherwise specified)

to sources measured in FUV and NUV with an accuracy better than 0.1 mag. We have checked that considering the whole sample of galaxies detected in FUV and NUV does not change the results, only adding a larger dispersion in the diagrams. Shown in Fig. 2 is a plot of  $L_{\text{IR}}/L_{\text{UV}}$  as a function of  $\beta$ , together with local relations for starbursts (Kong et al. 2004) and optically selected star-forming galaxies (Boissier et al. 2007) are superposed. Galaxies from our IR-selected sample exhibit a wide range of  $\beta$  and  $L_{\text{IR}}/L_{\text{UV}}$  values as already found in the nearby universe (Buat et al. 2005; Seibert et al. 2005; Takeuchi et al. 2010). The majority of the galaxies lie between the two relations i.e. have a dust attenuation (as defined by  $L_{\text{IR}}/L_{\text{UV}}$ ) for a given  $\beta$  that is larger than that found in local normal star-forming galaxies but lower than in local starbursts. From the 164 LIRGs of our initial sample of 1542 sources at  $z < 0.3$  in the Lockman SWIRE field, 125 are detected in NUV and FUV, of which 78 have a reliable estimate of  $\beta$  ( $\Delta m < 0.1$  mag in FUV and NUV) and are shown in Fig. 2. 67 of these 78 LIRGs (i.e. 87%) are found to lie below the local starburst relation. The fraction drops to 77% for the 125 LIRGs detected in both FUV and NUV without any restriction on the measurement accuracy. 11% of the galaxies (including 10 LIRGs) detected in NUV have no FUV detection (for these we adopt a limiting FUV magnitude of 24.8 (Morrissey et al. 2005) ; if we consider only sources with NUV magnitudes with  $\Delta NUV < 0.1$ , all these sources are found below the starburst law. This estimate might be uncertain given the large number of *GALEX* fields with different exposure times. As quoted in Section 2, 23% of the initial sample at  $z < 0.3$  is detected neither in NUV nor FUV: the limiting magnitude of  $NUV = 24.4$  roughly corresponds to a limit on  $L_{\text{IR}}/L_{\text{UV}}$  of  $\simeq 200$  in the redshift range  $0 < z < 0.3$  (for the lowest IR luminosities at each redshift). Therefore we miss at most 23% of galaxies with  $\log(L_{\text{IR}}/L_{\text{UV}}) > 2.3$  (note that fewer than 23% may be genuine non-detections as discussed for the Lockman North field). A detailed discussion of UV non-detections is deferred to a future paper. Nevertheless, even if we account for galaxies not detected in the NUV and FUV, a substantial fraction of all the IR-selected galaxies is found below the local starburst law. Dust attenuation in these galaxies is *overestimated* if the recipe for starburst galaxies based on the UV spectral slope is applied.

The most distant galaxies of our sample, including LIRGs, are found to depart strongly from the starburst law (see Fig. 2).  $\beta$  is calculated from the observed  $FUV - NUV$  colour: the wavelengths sampled go from 150 and 230 nm at  $z=0$  to 118 and 180 nm at  $z=0.3$ . Therefore, the power law model for the UV continuum assumed to calculate  $\beta$  might not be valid for the whole 118-230 nm range and for dust attenuations ranging from 0.5 to 5 mag in UV. The uncertainty can also be amplified because of the rather large bandwidths of the *GALEX* filters (Morrissey et al. 2005). Variations in dust properties and star versus dust geometry are known to induce large dispersions in the  $L_{\text{IR}}/L_{\text{UV}} - \beta$  diagram (Gordon et al. 2000; Boquien et al. 2009)). Our selection at  $250\mu\text{m}$  may also lead to more quiescent galaxies than local LIRGs in terms of star formation which is known to increase  $\beta$  for a given  $L_{\text{IR}}/L_{\text{UV}}$  (Kong et al. 2004). At  $z=2$  Reddy et al. (2010) found that Lyman Break Galaxies also detected at  $24\mu\text{m}$  and with bolometric luminosity lower than  $10^{12}L_{\odot}$  follow the local starburst law, although with a

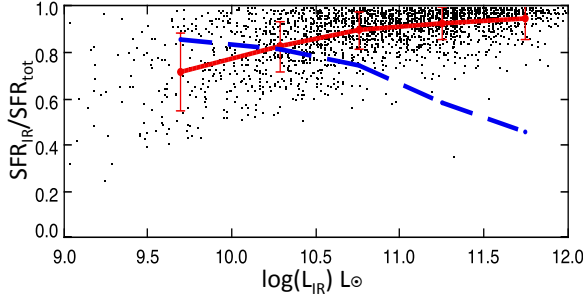


**Figure 3.** Fraction of SFR measured in IR,  $SFR_{IR}$  as a function of the IR luminosity,  $L_{IR}$ . The mean and standard deviation of the values in 5 bins of  $\log(L_{IR})$ :  $< 10$ ,  $10$ - $10.5$ ,  $10.5$ - $11$ ,  $11$ - $11.5$ ,  $> 11.5$  are shown in red, joined by a solid line to guide the eye. The blue dashed line represents the fraction of galaxies detected in the UV at each value of  $\log(L_{IR})$

large dispersion. These galaxies have  $\beta < -0.5$  and therefore are much bluer than the bulk of our sample. At high redshift the dynamical range in stellar population is narrower and the contribution to the UV continuum of stars not related to the current star formation is likely to be negligible in star forming galaxies at  $z > 1$ . The spatial distribution of dust and young stars may also be similar to that found in strong local starbursts making the law proposed by Meurer, Heckman, & Calzetti (1999) more appropriate for these high redshift objects than for our present sample.

This topic will be re-investigated in a future work by fitting the whole SED from the UV to the IR both at low and high redshift.

## 5 CALIBRATING MEASURES OF STAR FORMATION RATE

An important check is to test whether IR emission alone provides a robust estimate of the total SFR over the whole range of IR luminosities or if ignoring the direct UV light leads to systematic errors. We again use the sample derived from the Lockman-SWIRE field because of the large number of galaxies in the sample.

We take  $SFR_{IR} + SFR_{UV} = SFR_{tot}$  as a reference for the SFR measure where  $\log(SFR_{IR})_{M_{\odot}yr^{-1}} = \log(L_{IR})_{L_{\odot}} - 9.97$  and  $\log(SFR_{UV})_{M_{\odot}yr^{-1}} = \log(L_{UV})_{L_{\odot}} - 9.69$ . The UV emission is not corrected for dust attenuation and we use the SFR calibrations from Buat et al. (2008) with the assumption of a constant SFR over  $10^8$  years and a Kroupa initial mass function (Kroupa 2001).

Plotted in Fig. 3 is the SFR fraction measured by the IR luminosity,  $SFR_{IR}/SFR_{tot}$ , as a function of  $L_{IR}$ , with an additional curve showing the fraction of the galaxies in the sample with that IR luminosity that are detected in the UV. When the sample is considered as a whole, we find that  $SFR_{IR}$  measures  $\sim 90\%$  of the total SFR. This fraction

varies with  $L_{IR}$ : from  $94 \pm 10\%$  for the most luminous galaxies of our sample ( $L_{IR} > 10^{11.5} L_{\odot}$ ) with 45% detected in UV, down to  $71 \pm 17\%$  when  $L_{IR} < 10^{10} L_{\odot}$  or equivalently  $SFR_{tot} < 1 M_{\odot}yr^{-1}$  and a UV detection rate reaching 85%. This demonstrates that the combination of obscured and unobscured SFRs is required to determine accurate SFRs in galaxies with low star formation activity. Intrinsically faint galaxies detected in rest-frame UV surveys are found to be a significant component of luminosity functions and of the total star formation density at both low and high redshifts (Buat et al. 2007a; Reddy & Steidel 2009). As a consequence, both UV and IR selected samples must be built and their contribution added to measure the total star formation density at a given redshift (Iglesias-Páramo et al. 2006; Reddy & Steidel 2009).

Shown in Fig 4 is a comparison of the SFR measured in the UV with  $SFR_{tot}$ , for both uncorrected and corrected UV luminosities, where the correction used is that of Meurer, Heckman, & Calzetti (1999):  $A_{UV} = 4.43 + 1.99\beta$  deduced from their  $L_{IR}/L_{UV}$ - $\beta$  relation. For this correction we only consider galaxies with  $z < 0.2$  to narrow the wavelength range used to calculate  $\beta$ . Without dust attenuation corrections,  $SFR_{UV}$  underestimates the total SFR by a factor  $\sim 6$  for  $SFR_{tot} \simeq 1 M_{\odot}yr^{-1}$  and  $\sim 30$  for  $SFR_{tot} \simeq 100 M_{\odot}yr^{-1}$ . As expected from Fig 2, with dust corrections based on  $\beta$ , SFRs are overestimated by a factor  $\sim 2-3$ . At  $z \sim 1$  Elbaz et al. (2007) only obtain  $SFR \leq 10 M_{\odot}yr^{-1}$  when correcting UV luminosities for dust attenuation based on values of  $\beta$ . They use the  $U-B$  colour to measure  $\beta$  which corresponds to the wavelength range 180-225 nm at  $z \sim 1$ ; which is different from the ranges used in this work and by Meurer, Heckman, & Calzetti (1999). Burgarella et al. (2007) and Reddy & Steidel (2009) corrected UV measurements using the  $L_{IR}/L_{UV}$ - $\beta$  relation for local starbursts and found SFR deduced from UV-corrected luminosities to be in agreement with  $SFR_{tot}$  out to few 100s  $M_{\odot} yr^{-1}$ , albeit with significant dispersion. As discussed in section 4, this agreement is likely to be due to the different nature of UV selected galaxies at  $z > 1$  as compared to the IR selected galaxies analysed in the present work.

## ACKNOWLEDGEMENTS

SPIRE has been developed by a consortium of institutes led by Cardiff University (UK) and including Univ. Lethbridge (Canada); NAOC (China); CEA, OAMP (France); IFSI, Univ. Padua (Italy); IAC (Spain); Stockholm Observatory (Sweden); Imperial College London, RAL, UCL-MSSL, UKATC, Univ. Sussex (UK); and Caltech/JPL, IPAC, Univ. Colorado (USA). This development has been supported by national funding agencies: CSA (Canada); NAOC (China); CEA, CNES, CNRS (France); ASI (Italy); MCINN (Spain); SNSB (Sweden); STFC (UK); and NASA (USA). The data presented in this paper will be released through the *Herschel* Database in Marseille HeDaM (<http://hedam.oamp.fr/HerMES>) This work makes use of TOPCAT <http://www.star.bristol.ac.uk/~mbt/topcat/>.

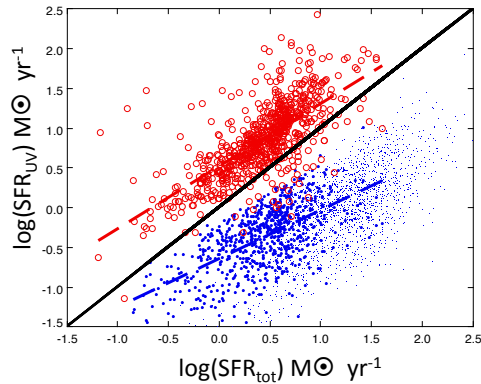


**Figure 4.** A plot of  $\text{SFR}_{\text{UV}}$  vs.  $\text{SFR}_{\text{tot}}$ , where  $\text{SFR}_{\text{tot}} = \text{SFR}_{\text{IR}} + \text{SFR}_{\text{UV}}$ . SFRs deduced from uncorrected UV fluxes are plotted with blue dots, the largest ones correspond to galaxies at  $z < 0.2$ . SFRs deduced from UV fluxes corrected for dust attenuation with the relation of Meurer, Heckman, & Calzetti (1999) are plotted with open green circles for galaxies with  $z < 0.2$ . The linear regression lines between  $\text{SFR}_{\text{tot}}$  and the two estimates of  $\text{SFR}_{\text{UV}}$  are plotted as dashed lines. The black solid line corresponds to equal values on both axes.

## REFERENCES

- Abazajian K. N., et al., 2009, ApJS, 182, 543  
 Boissier S., et al., 2007, ApJS, 173, 524  
 Boquien, M., Calzetti, D., Kennicutt, R. et al., 2009, ApJ, 706, 553  
 Buat, V. et al. 2005, ApJ, 619, L51  
 Buat, V., Takeuchi, T. T., Iglesias-Páramo, J, et al. 2007, ApJS, 173, 404  
 Buat, V., Marcellac, D., Burgarella, D. 2007, A&A, 469, 19  
 Buat, V., Boissier, S., Burgarella, D. et al. 2008, A&A, 483, 107  
 Burgarella, D., Le Floch, E., Takeuchi, T. T. 2007, MNRAS, 380, 986  
 Daddi E., et al., 2007, ApJ, 670, 156  
 Dale, D. A., Helou, G. 2002, ApJ, 576, 159  
 Elbaz, D., Daddi, E., Le Borgne, D. et al. 2007, A&A, 468, 33  
 Goldader J. D., Meurer G., Heckman T. M., Seibert M., Sanders D. B., Calzetti D., Steidel C. C., 2002, ApJ, 568, 651  
 Gordon K. D., Clayton G. C., Witt A. N., Misselt K. A., 2000, ApJ, 533, 236  
 Griffin, M. et al, A&A special issue  
 Iglesias-Páramo J., Buat V., Donas J., Boselli A., Milliard B., 2004, A&A, 419, 109  
 Iglesias-Páramo J., et al., 2006, ApJS, 164, 38  
 Kong X., Charlot S., Brinchmann J., Fall S. M., 2004, MNRAS, 349, 769  
 Kroupa P., 2001, MNRAS, 322, 231  
 Howell J. H., et al., 2010, ApJ, 715, 572  
 Martin D. C., et al., 2005, ApJ, 619, L1  
 Morissey, P. et al. 2005, ApJ, 619, L7  
 Meurer G. R., Heckman T. M., Calzetti D., 1999, ApJ, 521, 64

- Noll S., Burgarella D., Giovannoli E., Buat V., Marcellac D., Muñoz-Mateos J. C., 2009, A&A, 507, 1793  
 Oliver et al., 2010, in prep.  
 Pilbratt et al. A&A special issue  
 Poglitch, A. et al. A&A special issue  
 Reddy, N. A., Steidel, C. C., Pettini, M. et al. 2008, ApJ, 692, 778  
 Reddy N. A., Steidel C. C., 2009, ApJ, 692, 778  
 Reddy N. A., Erb D. K., Pettini M., Steidel C. C., Shapley A. E., 2010, ApJ, 712, 1070  
 Roseboom, I. et al, 2010, MNRAS, submitted  
 Rowan-Robinson M., et al., 2008, MNRAS, 386, 697  
 Siebenmorgen, R., Krügel, E. 2007, A&A, 461, 445  
 Seibert M., et al., 2005, ApJ, 619, L55  
 Strazzullo V., Pannella M., Owen F. N., Bender R., Morrison G. E., Wang W.-H., Shupe D. L., 2010, ApJ, 714, 1305  
 Takeuchi T. T., Buat V., Heinis S., Giovannoli E., Yuan F.-T., Iglesias-Páramo J., Murata K. L., Burgarella D., 2010, A&A, 514, A4  
 Xu, C.K., Shupe, D., Buat, V. et al. 2007, ApJS 173, 432  
 Zheng X. Z., Dole H., Bell E. F., Le Floch E., Rieke G. H., Rix H.-W., Schiminovich D., 2007, ApJ, 670, 301

This paper has been typeset from a  $\text{T}_{\text{E}}\text{X}/\text{L}^{\text{A}}\text{T}_{\text{E}}\text{X}$  file prepared by the author.